

See discussions, stats, and author profiles for this publication at: <https://www.researchgate.net/publication/231273116>

Asphaltene Molecular Size by Fluorescence Correlation Spectroscopy

ARTICLE *in* ENERGY & FUELS · JULY 2007

Impact Factor: 2.79 · DOI: 10.1021/ef700216r

CITATIONS

59

READS

18

4 AUTHORS, INCLUDING:



A. Ballard Andrews

Schlumberger Limited

67 PUBLICATIONS 1,273 CITATIONS

SEE PROFILE



Sudipa Mitra-Kirtley

Rose Hulman Institute of Technology

23 PUBLICATIONS 482 CITATIONS

SEE PROFILE



Oliver C Mullins

Schlumberger Limited

244 PUBLICATIONS 5,940 CITATIONS

SEE PROFILE

Asphaltene Molecular Size by Fluorescence Correlation Spectroscopy

Marc H. Schneider,^{†,‡} A. Ballard Andrews,^{*,†} Sudipa Mitra-Kirtley,[‡] and Oliver C. Mullins[†]

Schlumberger-Doll Research, Cambridge, Massachusetts 02139, and Rose-Hulman Institute of Technology, Terre Haute, Indiana 47803

Received April 26, 2007. Revised Manuscript Received June 20, 2007

Asphaltene molecular size and weight have been of concern since asphaltenes were first isolated from crude oils. Despite previous divergent results on this topic, in recent years, there has been a growing consensus among all mass spectral ionization techniques and all diffusion measurements that asphaltenes are fairly small molecules. In this paper, fluorescence correlation spectroscopy (FCS) is used to determine translational diffusion coefficients of asphaltene and model compounds under a variety of conditions. These FCS studies provide several stringent tests on asphaltene molecular size and architecture. A broad range of concentrations including ultralow concentrations is investigated to ensure the lack of potential aggregation difficulties. Large temperature variations are used to test the application of the simple diffusion equation. FCS results here clearly show the dependence of the diffusion constant on the molecular weight. Finally, FCS results on asphaltenes are in quantitative agreement with those of time-resolved fluorescence depolarization on asphaltenes. A comparison of the results herein with previous FCS and time-resolved fluorescence depolarization (TRFD) results on the same asphaltenes confirms the correlation between molecular size and asphaltene chromophore size; this supports a molecular architecture with one or two polycyclic aromatic hydrocarbons (PAHs) per molecule and counters proposed structures with many PAHs per asphaltene molecule.

1. Introduction

Asphaltenes^{1–3} represent an important class of crude oils and constitute a large mass fraction of heavy oils, which are expected to be increasingly used. Asphaltenes are important players in all aspects of hydrocarbon resource use. To improve corresponding efficiencies, it is essential to understand the asphaltene molecular structure.¹ Asphaltenes, the most aromatic and enigmatic component of crude oil, are defined as a solubility class (e.g., toluene soluble and *n*-heptane insoluble); their chemical identity has been elusive. The most important attribute of any chemical substance is its elemental composition. Fortunately, there is no debate about this issue for asphaltenes; albeit, asphaltenes from different sources or isolated using different processes do exhibit differences even in elemental composition. The second most important attribute of any chemical substance is its molecular weight. Asphaltenes have been able to ignite considerable controversy here. Initial results from field ionization mass spectroscopy (FIMS) showed that asphaltenes have a centroid molecular weight of ~800 Da (Daltons = g/mol) with considerable width to this distribution.⁴ In mass spectroscopy, the ionization method is always of considerable concern and can introduce artifacts or biases if not performed correctly. Consequently, it is essential to test a variety of ionization methods. Atmospheric pressure photoionization (APPI)⁵ and atmospheric pressure chemical ionization (APCI)⁶

gave results consistent with the FIMS results. More recently, electrospray ionization, Fourier transform ion cyclotron resonance mass spectroscopy (ESI–FTICR–MS) has been applied to asphaltenes and found that the most abundant species are between 400 and 800 Da, with all species being below 2000 Da.⁷ Laser desorption ionization (LDI), including matrix-assisted laser desorption ionization, has given inconsistent results in the literature. However, recent work has established that LDI gives artificially high molecular weights if either the laser power is too high, the asphaltene surface concentration is too high, or the ions are extracted continuously.⁸ These artifacts are likely the source of discrepancies noted in the literature.⁹

A separate line of investigation of the asphaltene molecular weight and size involves the determination of the asphaltene molecular diffusion coefficient. The first diffusion measurements of asphaltenes used time-resolved fluorescence depolarization (TRFD)^{10–14} to measure rotational diffusion coefficients. These studies obtained the result that asphaltene molecular weights are ~750 Da, with a range of 500–1000 Da for the bulk of the population. Thus, the TRFD diffusion measurements are in close

* To whom correspondence should be addressed. Fax: 617-768-2384. E-mail: bandrews@slb.com.

[†] Schlumberger-Doll Research.

[‡] Rose-Hulman Institute of Technology.

(1) *Asphaltenes, Heavy Oils, and Petroleomics*; Mullins, O. C., Sheu, E. Y., Hammami, A., Marshall, A. G., Eds.; Springer: New York, 2006.

(2) *Structures and Dynamics of Asphaltenes*; Mullins, O. C., Sheu, E. Y., Eds.; Plenum Press: New York, 1998.

(3) *Chemistry of Asphaltenes*; Bunger, J. W., Li, N. C., Eds.; American Chemical Society: Washington, D.C., 1984.

(4) Boduszynski, M. M. Asphaltenes in petroleum asphalt: Composition and formation. In *Chemistry of Asphaltenes*; Bunger, J. W., Li, N. C., Eds.; American Chemical Society: Washington, D.C., 1984; Chapter 7.

(5) Merdrignac, I.; Desmazieres, B.; Terrier, P.; Delobel, A.; Laprevote, O. Analysis of raw and hydrotreated asphaltenes using off-line and on-line SEC/MS coupling. Proceedings of Heavy Organic Deposit, Los Cabos, Mexico, 2004.

(6) Cunico, R. I.; Sheu, E. Y.; Mullins, O. C. Molecular weight measurement of UG8 asphaltene by APCI mass spectroscopy. *Pet. Sci. Technol.* **2004**, 22 (7–8), 787–798.

(7) Rodgers, R. P.; Marshall, A. G. Petroleomics: Advanced characterization of petroleum-derived materials by Fourier transform ion cyclotron resonance mass spectrometry. In *Asphaltenes, Heavy Oils, and Petroleomics*; Mullins, O. C., Sheu, E. Y., Hammami, A., Marshall, A. G., Eds.; Springer: New York, 2006; Chapter 3.

(8) Hortal, A. R.; Martinez-Haya, B.; Lobato, M. D.; Pedrosa, J. M.; Lago, S. On the determination of molecular weight distributions of asphaltenes and their aggregates in laser desorption ionization experiments. *J. Mass Spectrom.* **2006**, 41, 960.

(9) Mullins, O. C. Rebuttal to comment by Professors Herod, Kandiyoti, and Bartle on molecular size and weight of asphaltene and asphaltene solubility fractions from coals, crude oils and bitumen by S. Badre, C. C. Goncalves, K. Norinaga, G. Gustavson, and O. C. Mullins. *Fuel* **2006**, 85, 1–11. *Fuel*, manuscript accepted.

accordance with the mass spectral results. In addition, TRFD was employed to show that coal asphaltene are significantly smaller than petroleum asphaltene.^{11–14} The explanation was given that coal asphaltene lacking alkanes exhibit less steric repulsion; thus, they must have smaller fused aromatic ring systems to balance intermolecular repulsion and attraction. This explains the known smaller fused aromatic ring systems for coal asphaltene.¹³ The small alkane fraction coupled with small fused ring systems makes for smaller molecules for coal asphaltene. The confirmation of the small size of coal asphaltene has been obtained by Taylor dispersion measurements;¹⁵ these studies report almost the same exact size for the same asphaltene as TRFD studies.¹⁵ Nuclear magnetic resonance (NMR) diffusion measurements obtain a similar but slightly larger centroid for asphaltene molecular size.¹⁶ This reasonable agreement by a very different method is welcome. The slightly larger molecular sizes found in the NMR studies may be due to some dimer formation. The lowest concentrations employed in the NMR studies (50 mg/L) are comparable to those where dimer formation is thought to initiate.¹⁷ At somewhat higher concentrations, nanoaggregation occurs as shown by high-Q ultrasonics¹⁸ and the same NMR study.¹⁶

Fluorescence correlation spectroscopy (FCS) has been employed to study the translational diffusion of asphaltene molecules.^{19,20} FCS measures translation diffusion coefficients by monitoring the decay of the fluorescence autocorrelation function versus time. The FCS results reported for petroleum¹⁹ and coal²⁰ asphaltene are in reasonable agreement with results reported by TRFD. The results for the coal asphaltene are somewhat lower by FCS than TRFD. The coal asphaltene rotational diffusion coefficients are at the lower limit for TRFD studies¹¹ but are easily measured by FCS.²⁰ Also, the determination of molecular radii from translation and rotational diffusion coefficients depends differently upon molecular asymmetry. This issue has been reviewed for asphaltene in detail for rotational diffusion coefficients,^{10,12} and the effect is not large. For translation diffusion coefficients, this might be a more serious issue.¹⁶

In general, for asphaltene, the FCS results do show slightly smaller asphaltene molecular sizes than the TRFD results. A significant factor is the different spectral ranges employed in

the FCS versus TRFD studies. The TRFD studies use lasers of different wavelengths from ~360 to 660 nm. All TRFD studies show a large increase in molecular size with an increasing wavelength. It is known that larger polycyclic aromatic hydrocarbons (PAHs) of asphaltene absorb at longer wavelengths.^{21–23} This result is expected from the familiar quantum particle-in-a-box and has been established by exhaustive molecular orbital calculations on PAHs.^{21–23} The TRFD studies show that the short wavelengths employed by the FCS studies will emphasize smaller asphaltene molecules. Furthermore, the quantum yields of these smaller, blue-emitting molecules are larger, reinforcing this selection.²⁴ Nevertheless, the TRFD studies, which have been shown to be consistent with the FCS results,^{19,20} are performed at long wavelengths to capture the small quantum yield components of crude oils.^{10–14} Consequently, fluorescence diffusion measurements do give representative results for asphaltene.

An important implication about the small molecular weight of asphaltene is that they have, for the most part, one PAH ring system per molecule. We do note that some molecules with a pendant group with a benzene ring or naphthalene would not have a large impact on the diffusion measurements. Analysis of the absorption and emission spectra of asphaltene by molecular orbital (MO) calculations shows that the asphaltene PAHs possess seven fused rings on average.²¹ This is in close agreement with all TRFD diffusion measurements of (petroleum) asphaltene molecular size.^{10–14,21} This is also in accordance with direct molecular imaging studies of asphaltene by scanning tunneling microscopy²⁵ and high-resolution transmission electron microscopy.²⁶ With seven fused rings and the roughly 60% alkane carbon of petroleum asphaltene, one accounts for ~700 Da with a single fused ring system. This explains why there is a factor of 10 variation of the asphaltene molecular volume with the excitation (and emission) wavelength. The asphaltene chromophore accounts for a significant fraction (~1/2) of the molecular size. Small, blue-emitting chromophores constitute small asphaltene molecules, while large, red-emitting chromophores constitute large asphaltene molecules. MO calculations of the red absorption edge of asphaltene support this contention.²⁷

There has been some question as to whether asphaltene molecules fluoresce sufficiently for fluorescence methods to be employed. First, by selecting the pair of wavelengths for optical excitation and fluorescence emission, one can analyze asphaltene molecular populations of low quantum yield without interference from highly fluorescent asphaltene molecular classes.^{10–14} Second, the quantum yield of asphaltene shows large, wavelength-dependent variability and indeed does get small at long wavelengths.²⁴ This is a natural consequence of the Energy Gap Law familiar in the spectroscopy of crude oils.²⁴ However, even at very long wavelengths, the asphaltene and crude oil quantum yields are nonzero; fluorescence techniques employing lasers can be used effectively. Third, claims that asphaltene fractions

(10) Groenzin, H.; Mullins, O. C. Asphaltene molecular size and structure. *J. Phys. Chem. A* **1999**, *103*, 11237.

(11) Groenzin, H.; Mullins, O. C. Molecular sizes of asphaltene from different origin. *Energy Fuels* **2000**, *14*, 677.

(12) Groenzin, H.; Mullins, O. C. Asphaltene molecular size and weight by time-resolved fluorescence depolarization. In *Asphaltene, Heavy Oils, and Petrochemicals*; Mullins, O. C., Sheu, E. Y., Hammami, A., Marshall, A. G., Eds.; Springer: New York, 2006; Chapter 2.

(13) Buenrostro-Gonzalez, E.; Groenzin, H.; Lira-Galeana, C.; Mullins, O. C. The overriding chemical principles that define asphaltene. *Energy Fuels* **2001**, *15*, 972.

(14) Badre, S.; Goncalves, C. C.; Norinaga, K.; Gustavson, G.; Mullins, O. C. Molecular size and weight of asphaltene and asphaltene solubility fractions from coals, crude oils and bitumen. *Fuel* **2006**, *85*, 1–11.

(15) Wargadalam, V. J.; Norinaga, K.; Iino, M. Size and shape of a coal asphaltene studied by viscosity and diffusion coefficient measurements. *Fuel* **2002**, *81*, 1403.

(16) Freed, D. E.; Lisitz, N. V.; Sen, P. N.; Song, Y.-Q. Molecular composition and dynamics of oils from diffusion measurements. In *Asphaltene, Heavy Oils, and Petrochemicals*; Mullins, O. C., Sheu, E. Y., Hammami, A., Marshall, A. G., Eds.; Springer: New York, 2006; Chapter 11.

(17) Goncalves, S.; Castillo, J.; Fernandez, A.; Hung, J. Absorbance and fluorescence spectroscopy on the aggregation behavior of asphaltene-toluene solutions. *Fuel* **2004**, *83*, 1823.

(18) Andreatta, G.; Bostrom, N.; Mullins, O. C. High-Q ultrasonic determination of the critical nanoaggregate concentration of asphaltene and the critical micelle concentration of standard surfactants. *Langmuir* **2005**, *21*, 2728–2736.

(19) Andrews, A. B.; Guerra, R. E.; Mullins, O. C.; Sen, P. N. Diffusivity of asphaltene molecules by fluorescence correlation spectroscopy. *J. Phys. Chem. A* **2006**, *110*, 8093.

(20) Guerra, R.; Andrews, A. B.; Ladavac, K.; Mullins, O. C.; Sen, P. N. Diffusivity of coal and petroleum asphaltene monomers by fluorescence correlation spectroscopy. **2007**, manuscript to be published in *Fuel*.

(21) Ruiz-Morales, Y.; Mullins, O. C. Polycyclic aromatic hydrocarbons of asphaltene analyzed by molecular orbital calculations with optical spectroscopy. *Energy Fuels* **2007**, *21*, 256.

(22) Ruiz-Morales, Y. *J. Phys. Chem. A* **2002**, *106*, 11283.

(23) Ruiz-Morales, Y. Molecular orbital calculations and optical transitions of PAHs and asphaltene. In *Asphaltene, Heavy Oils, and Petrochemicals*; Mullins, O. C., Sheu, E. Y., Hammami, A., Marshall, A. G., Eds.; Springer: New York, 2006; Chapter 4.

(24) Ralston, C. Y.; Wu, X.; Mullins, O. C. Quantum yields of crude oils. *Appl. Spectrosc.* **1996**, *50*, 1563.

(25) Zajac, G. W.; Sethi, N. K.; Joseph, J. T. *Scanning Microsc.* **1994**, *8*, 463.

(26) Sharma, A.; Groenzin, H.; Tomita, A.; Mullins, O. C. Probing order in asphaltene and aromatic ring systems by HRTEM. *Energy Fuels* **2002**, *16*, 490.

(27) Ruiz-Morales, Y.; Wu, X.; Mullins, O. C. Electronic absorption edge of crude oils and asphaltene analyzed by molecular orbital calculations with optical spectroscopy. *Energy Fuels* **2007**, *21*, 944–952.

do not fluoresce have suffered from aggregation effects (cf. ref 9 and references therein with ref 14). It is well-known that aggregation can quench fluorescence of asphaltenes as well as laser dyes.² FCS methods employ exceedingly low concentrations (as low as 23 $\mu\text{g/L}$ for asphaltenes) and are shown herein not to suffer from aggregation effects. Fourth, quenching is accompanied by fluorescence lifetime reduction because of the additional decay (quenching) mechanism. Asphaltenes in dilute solution do not exhibit significantly shorter fluorescent lifetimes than maltenes for given wavelengths; thus, it is likely that asphaltenes do not possess additional quenching mechanisms.²⁸ Fifth, we have measured molecular diffusion coefficients in the spectral ranges where asphaltenes exhibit primary optical absorption.²¹ Consequently, we believe that we are measuring asphaltene molecular sizes for all classes of asphaltene molecules. The possibility that there is a class of asphaltene molecules with very different molecular weight that do not fluoresce, do not appear in NMR diffusion⁹ measurements (no hydrogen), are not detected by optical absorption in Taylor diffusion measurements (no color), and do not show up in any mass spectral technique is simply untenable.

In this study, we employ FCS methods to determine translational diffusion coefficients of asphaltenes. A comparison of these diffusion coefficients with a variety of model compounds is made. To obtain reliably subtle differences in these diffusion coefficients, a new optical train was fabricated and is shown to work with high accuracy. Large variations of concentrations are employed to rule out artifacts. Subtle differences in the chemistry of petroleum asphaltenes have been shown to impact molecular sizes and thus diffusion coefficients. A corroboration of previous results is found here, reinforcing that diffusion measurements of asphaltenes offer a sensitive and powerful probe of asphaltene molecular structure.

2. Theory

Spontaneous fluctuations are present in every fluorescence measurement. Although these fluctuations are either too fast to be seen or appear as noise in traditional fluorescence measurements, FCS extracts information from these fluctuations by quantifying their strength and duration with temporal autocorrelation of the recorded intensity signal. The fluctuations result from fluorescent molecules diffusing into or out of the focal volume of solution interrogated in the FCS experiment. These fluctuations in the fluorescence signal can be expressed as²⁹

$$\delta F(t) = \eta \int_{\mathcal{V}} W(\vec{r}) \delta C(\vec{r}, t) dV \quad (1)$$

where $W(\vec{r})$ is the normalized point spread function (PSF) and $\delta C(\vec{r}, t)$ describes the local concentration of the sample molecules. The factors for the overall detection efficiency, the molecular absorption cross-section, the fluorescence quantum yield, and the excitation intensity amplitude are assumed to be time-invariant, grouped together, and represented by the parameter η . For the assumption of a three-dimensional Gaussian probe volume, the normalized PSF can be written as $W(\vec{r}) = \exp[-2(x^2 + y^2)r_0^{-2} - 2z^2z_0^{-2}]$, where r_0 and z_0 are the radial and axial distance from the center to where the intensity has decayed by $1/e^2$, respectively.³⁰

(28) Ralston, C. Y.; Mitra-Kirtley, S.; Mullins, O. C. Small population of one to three fused-ring aromatic molecules in asphaltenes. *Energy Fuels* **1996**, *10*, 623.

(29) Schwille, H.; Haubein, P.; Haubein, E. Fluorescence correlation spectroscopy—An introduction to its concepts and applications. *Biophysics Textbook Online*, www.biophysics.org/btol/ (accessed January 2007).

(30) Lamb, D. C. Fundamentals of fluctuation spectroscopy. I: The basics of fluorescence correlation spectroscopy. Lecture notes on fluctuation spectroscopy, Department of Physical Chemistry, Ludwig-Maximilians-Universität (LMU), Munich, Germany, 2004.

The particle concentration $C(\vec{r}, t)$ can be described by the diffusion equation for a freely diffusing species

$$\frac{\partial}{\partial t} C(\vec{r}, t) = D \nabla^2 C(\vec{r}, t) \quad (2)$$

where D is the diffusion coefficient and ∇^2 is the Laplace operator.

The normalized autocorrelation function (ACF) for processes, which are both stationary and ergodic, is given by³⁰

$$G(\tau) = \frac{\langle \delta F(0) \delta F(\tau) \rangle}{\langle F \rangle^2} \quad (3)$$

where $\langle \rangle$ denotes the time average.

Using the cylindrical-shaped volume approximation for the effective focal volume $V_{\text{eff}} = (\int \hat{W}(\vec{r}) dV)^2 (\int \hat{W}^2(\vec{r}) dV)^{-1}$, the diffusion time $\tau_D = r_0^2/4D$, the aspect ratio $\beta = r_0/z_0$, and the relation between the particle number N and the concentration $\langle N \rangle = V_{\text{eff}} \langle C \rangle$, eq 3 can be evaluated together with eqs 1 and 2 to²⁹

$$G(\tau) = \frac{1}{\langle N \rangle} \frac{1}{1 + \frac{\tau}{\tau_D}} \frac{1}{\sqrt{1 + \beta^2 \frac{\tau}{\tau_D}}} \quad (4)$$

Equation 4 is used to model the acquired FCS data.

Once the diffusion coefficient of a molecule for a certain solvent is known, the hydrodynamic radius, which will give an estimate of the size of the molecule, can be calculated according to the Stokes–Einstein relation^{31,32}

$$R_H = \frac{k_B T}{6\pi\eta_s D} \quad (5)$$

where k_B is the Boltzmann constant, T is the absolute temperature, and η_s is the viscosity of the solvent. This relationship was published by Einstein in 1905³² to describe the movements of spherical particles with radius R_H suspended in a fluid as a result of Brownian motion. However, eq 5 can be applied for arbitrarily shaped particles, such as molecules, for which R_H then describes an equivalent radius of a sphere with the same diffusion properties.

3. Experimental Section

Figure 1 shows a schematic of the FCS microscope used in this project. The excitation light was provided by an air-cooled Ar ion laser from JDS Uniphase with a 25 mW multiline laser head. The wavelength that we chose for this experiment was the 515 nm laser line. The laser light was connected to the optical train via a single-mode fiber and fiber couplers. If accurately aligned, a single-mode fiber allows for only the propagation of a Gaussian TEM_{0,0} mode, creating a Gaussian beam shape at the output³³ and serving as a spatial filter for the excitation light. The fluorescent light on the emission side of the setup was coupled into a multimode fiber with a core diameter of 50 μm , which substitutes for a 50 μm pinhole. The multimode fiber was coupled to a cubic beam splitter, with each branch going to an avalanche photodiode (APD, Pacer). The

(31) Lakowicz, J. R. *Principles of Fluorescence Spectroscopy*, 2nd ed.; Kluwer Academic/Plenum Publishers: New York, 1999.

(32) Einstein, A. Über die von der molekularkinetischen Theorie der Wärme geforderte Bewegung von in ruhenden Flüssigkeiten suspendierten Teilchen. *Ann. Phys.* **1905**, *322*, 549–560.

(33) Boeckem, B. High-accuracy alignment based on atmospheric dispersion—Technological approaches and solutions for the dual-wavelength transmitter. Proceedings of IWAA 1999: 6th International Workshop on Accelerator Alignment; European Synchrotron Radiation Facility (ESRF), Grenoble, France, 1999.

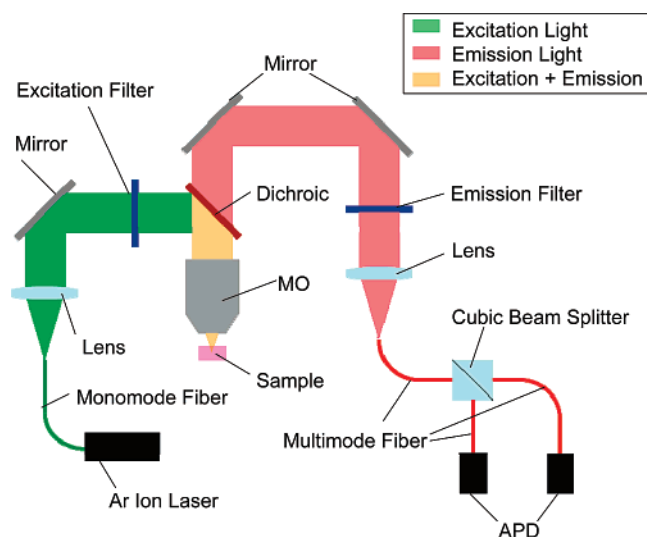


Figure 1. Schematic of the FCS microscope. The 515 nm Ar laser is coupled via a single-mode fiber to the optical train and collimated to slightly underfill the back aperture of the 60 \times objective. Cross-correlation is obtained with a beam splitter and two APDs.

two APDs were cross-correlated, yielding an improved signal. The maximum count rate for these single-photon counting modules was 5×10^6 cps with a dead time of 10 ns after each count. The optical train was built using components of the Microbench system (Linco), mounted on an optical breadboard. The microscope objective was a 60 \times oil immersion objective from Olympus, with a transmittance greater than 85% in the relevant wavelength range between 500 and 700 nm. The filter set used in the FCS microscope consisted of a narrow band-pass excitation filter for the 515 nm laser line (Edmund Optics), a dichroic (Chroma Technologies), and a Raman edge emission filter (CVI Laser).

Seven different petroleum asphaltenes were studied: CAL, Kuhm, AMH, UG8, K4A, BG5, and ST1, as well as an asphaltene extracted from coal. To establish a comparative scale for the asphaltene diffusion times, a selection of different model compounds was measured. A list of these dyes with their abbreviation, full name, chemical structure, and molecular weight is given in Table 1. The porphyrin TTB had the fastest diffusion time and provided a lower reference bound. The perylene derivatives BPTD, Solar-dye, and BPTI are molecules with a similar aromatic ring core system but different sized substituents. The cyanine derivative DTCP contains polar elements. The quantum dots (QDs) have a hydrodynamic radius of about 48 Å in toluene^{34,35} and provided an upper bound on the asphaltene molecular size.

The radial beam waist and the aspect ratio were determined from calibration measurements of the QD to be $r_0 = 430$ nm and $\beta = 0.1$, respectively. The room temperature was monitored and kept constant at $T = 290$ K during the experiments; therefore, the toluene viscosity was $\eta_s = 0.588$ cP at an ambient pressure of 14.7 psi.³⁶

Each sample was measured for at least two different concentrations to increase the confidence in the acquired values. The typical concentrations used for the asphaltene samples were 230 and 2300 $\mu\text{g/L}$. In general, coverage of 3 orders of magnitude in concentration by the FCS microscope was possible; therefore, a few samples such as the asphaltene K4A were measured at concentrations between

23 and 2300 $\mu\text{g/L}$. The perylene derivative BPTI, which has a very high molecular brightness, was measured at four different concentrations between 0.023 and 230 $\mu\text{g/L}$.

To check that the FCS data was indeed being interpreted correctly as molecular translational diffusion, we checked the temperature dependence as given by the Stokes–Einstein in eq 5. A Peltier element (Melcor) with a maximum heating/cooling power of 72 W was integrated in the sample holder. To prevent backscattering of excitation light into the microscope objective, the bottom surface of the sample slide was coated with a matt black paint.

4. Results and Discussion

Figure 2 shows an example of the raw (circles) and fitted data (solid lines) for the BPTD dye, at three different concentrations. The number of particles N scales as expected, but the diffusion time τ_D is identical for all three concentrations, giving added confidence in the data and verifying that no dimerization is occurring at the higher concentration. Figure 3 shows the FCS correlation curves for a series of model compounds, for several asphaltenes and QDs. The correlation functions are scaled so that the initial amplitudes $G(0)$ are the same for all curves. As noted in the Experimental Section, all of these curves are exactly fit by the theoretical formalism. The asphaltenes are essentially within the range of the model compounds and are much smaller than the rather large QDs. The perylene derivatives: BPTD, Solar, and BPTI have the same aromatic seven-ring core but differ only in the substituents. In addition, the diffusion coefficients decrease with an increasing molecular weight.

Asphaltenes in toluene have been shown to form nanoaggregates at low concentrations¹⁸ (150 mg/L) and dimers at lower concentrations¹⁷ (50 mg/L). FCS is applicable at very low concentrations as shown with the model compound in Figure 2. The concentration dependence of the FCS results was checked for several samples. Table 2 lists the results, with uncertainties propagated from the uncertainties of the curve fits and uncertainties in temperature and viscosity. The asphaltene diffusion coefficients are seen to be independent of the concentration at these low concentrations (~ 0.2 – 2 mg/L for petroleum asphaltenes), which are much lower than the concentrations where dimers are thought to form (~ 50 mg/L). Consequently, it is very likely that asphaltenes are molecularly dispersed in a true solution at these concentrations.

From eq 5, temperature is expected to have a large, predictable effect on the molecular diffusion process. In addition to the direct dependence on temperature, there is an indirect yet large effect through the solvent viscosity. Consequently, analyzing FCS data on asphaltenes in a large temperature range provides a stringent test of both the acquisition and interpretation of FCS data on asphaltenes.

The viscosity of toluene can be determined according to eq 6³⁶

$$\eta_s(T) = \frac{\eta_s^*}{6.035 \times 10^8 \left(\frac{M_{\text{Tol}}}{\rho_s} \right)^{2/3} (M_{\text{Tol}} RT)^{-0.5}} \quad (6)$$

where η_s^* , ρ_s , R , and T are the dimensionless viscosity, the density of the solvent, the gas constant, and the absolute temperature of the solvent, respectively. $M_{\text{Tol}} = 0.09214$ kg/mol is the molar mass of toluene.

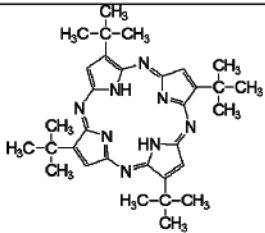
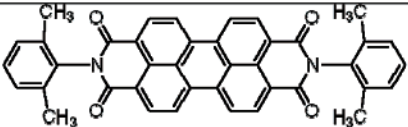
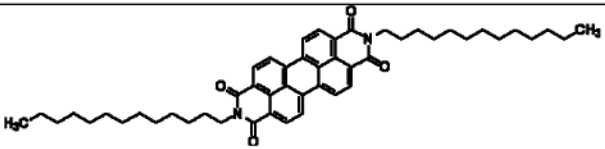
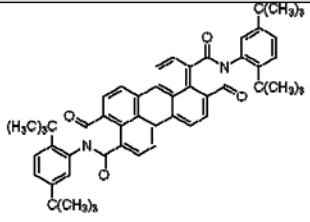
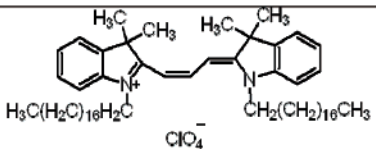
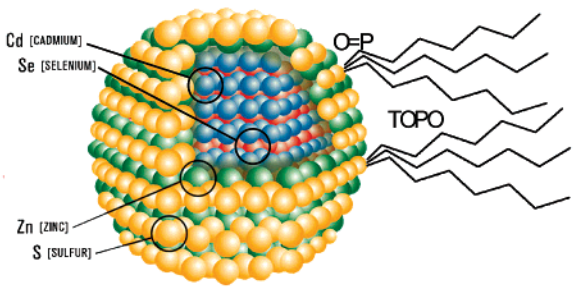
Figure 4a shows the variation of the calculated diffusion coefficient from FCS data versus the temperature for BG5 asphaltene. A monotonic variation of the diffusion coefficient is noted with a change of a factor of 2. Using eq 6 to account for the change in solvent viscosity with temperature in eq 5,

(34) Liedl, T.; Simon, K.; Simmel, F. C.; Rädler, J. O.; Parak, W. J. Fluorescent nanocrystals as colloidal probes in complex fluids measured by fluorescence correlation spectroscopy. *Small* **2005**, *1*, 997–1003.

(35) Pons, T.; Tetsuo Uyeda, H.; Medintz, I. L.; Mattoussi, H. Hydrodynamic dimensions, electrophoretic mobility, and stability of hydrophilic quantum dots. *J. Phys. Chem. B* **2006**, *110*, 20308–20316.

(36) Assael, M. J.; Avelino, H. M. T.; Dalaouti, N. K.; Fareleira, J. M. N. A.; Harris, K. R. Reference correlation for the viscosity of liquid toluene from 213 to 373 K at pressures to 250 MPa. *Int. J. Thermophys.* **2001**, *22*, 789–799.

Table 1. Fluorescent Dyes Used as Model Compounds for This Study

full name (abbreviation)	molecular structure	molecular weight (Da)
2,7,12,17- tetra-tert-butyl- 5,10,15,20-tetraaza- 21H,23H-porphine (TTB)		538.73
<i>N,N'</i> -bis(2,6- dimethylphenyl) perylene- 3,4,9,10-tetracarboxylic diimide (BPTD)		598.65
<i>N,N'</i> -ditridecylperylene- 3,4,9,10-tetracarboxylic diimide (Solar)		755.04
<i>N,N'</i> -bis(2,5-di-tert- butylphenyl)-3,4,9,10- perylenedicarboximide (BPTI)		766.96
1,1'-dioctadecyl-3,3,3',3'- tetramethylindocarbocyanine perchlorate (DTCP)		933.87
CdSe/ZnS core-shell crystal, type: Maple Red-Orange, TOPO capped (QD)		~200 000

the asphaltene molecular diameter can be derived for BG5 (Figure 4b). The near invariance of the derived molecular diameter versus temperature gives confirmation that the Stokes–Einstein equation correctly describes the diffusion kinetics. The 10% change in the derived molecular diameter might be an artifact but could also be associated with a subtle change in the molecular configuration at elevated temperatures. Note that this diameter corresponds to the specific chromophores excited by the excitation and emission wavelengths employed herein.

Table 3 compares the derived molecular diameter from FCS and TRFD of the QDs, two similar porphyrins, and asphaltenes for two different wavelengths. As expected, the QD and porphyrin diameters are independent of the excitation wavelength, because there is only one molecular component in these pure compounds. However, any asphaltene is a mixture of compounds. The different excitation wavelengths sample a different molecular component with differing molecular diameters as seen in Table 3. Furthermore, the longer wavelength component is comprised of larger molecules. This is born out

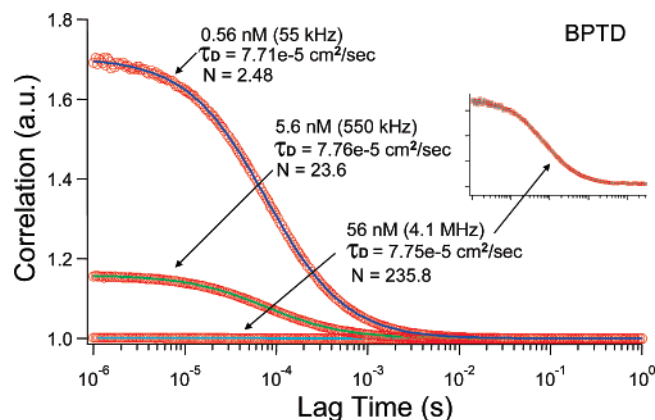


Figure 2. FCS data (markers) and the corresponding theoretical fit (solid lines) for three concentrations of BPTD, a perylene derivative. In the third generation of our FCS instrument, the experimental data and the corresponding fit (eq 4) are nearly indistinguishable. This superb fit to the data adds significant robustness to the results. The inset shows a close-up of the 56 nM concentration.

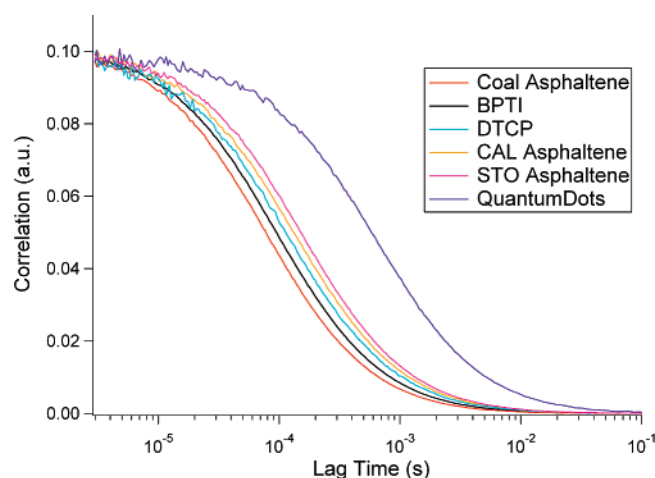


Figure 3. FCS correlation decay curves for several asphaltenes, model compounds, and QDs. The curves have been scaled along the y axis for display purposes. The model compounds provide upper and lower reference bounds for the range of possible asphaltene molecular sizes.

Table 2. Diffusion Times Were Obtained from Least-Squares Fits to the Data Using Eq 4 as the Fitting Function^a

sample name	diffusion time ($\times 10^{-5}$ s)	diffusion coefficient ($\times 10^{-6}$ cm ² /s)	hydrodynamic radius (Å)
coal, asphaltene	7.60 ± 0.04	6.06 ± 0.03	5.95 ± 0.04
BPTD, dye	7.73 ± 0.06	5.98 ± 0.04	6.05 ± 0.05
TTB, dye	7.87 ± 0.20	5.88 ± 0.15	6.15 ± 0.16
Solar, dye	9.41 ± 0.09	4.91 ± 0.05	7.36 ± 0.07
BPTI, dye	9.43 ± 0.06	4.90 ± 0.03	7.37 ± 0.05
DTCP, dye	11.2 ± 0.14	4.11 ± 0.05	8.79 ± 0.11
CAL, asphaltene	13.1 ± 0.23	3.52 ± 0.06	10.28 ± 0.18
Kuhm, asphaltene	13.8 ± 0.17	3.34 ± 0.04	10.82 ± 0.14
AMH, asphaltene	13.9 ± 0.08	3.34 ± 0.02	10.84 ± 0.07
UG8, asphaltene	14.5 ± 0.06	3.19 ± 0.02	11.34 ± 0.06
K4A, asphaltene	14.6 ± 0.10	3.16 ± 0.02	11.45 ± 0.09
BG5, asphaltene	14.7 ± 0.08	3.15 ± 0.02	11.48 ± 0.07
ST1, asphaltene	15.1 ± 0.12	3.05 ± 0.02	11.84 ± 0.10
quantum dots	60.8	0.76×10^{-6}	47.78

^a The diffusion coefficients were then derived from $\tau_D = r_0^2/4D$, and the hydrodynamic radii were derived from eq 5. The excitation source was the 514 nm wavelength line from an Ar laser.

in experiments^{10–14} and theory.²¹ According to MO calculations, the ring systems sampled by the excitation and emission wavelengths used here should sample fused ring systems with

approximately eight rings, whereas the data from ref 20 in Table 2 should sample fused ring systems with approximately five rings.

“Island” Molecular Model versus “Archipelago” Molecular Model. The molecular architecture of asphaltenes has been subject to much debate. The FCS data presented here support an asphaltene molecular architecture that has predominantly one or perhaps sometimes two PAHs per molecule. A molecule with many PAHs (generally the archipelago model) is refuted. We note that a molecule with a single large PAH but which has a pendant substituent with a phenyl or a naphthyl group would be compatible with our data. First, for several petroleum asphaltenes (CAL, ST1, and UG8), the molecular sizes for this spectral range for TRFD and FCS are in close agreement as shown in Table 3. This confirms that the rotational diffusion measurements of TRFD are not perturbed by internal rotation because internal rotation would have zero impact on the determination of translational diffusion coefficients via FCS. Second, TRFD results on rotational molecular diffusion^{10–14} showed a large (order of magnitude) dispersion of rotational correlation time versus emission wavelength. This was attributed to the huge color dependence of PAH chromophores of different size. Asphaltene molecules with a small PAH emit blue light and undergo fast diffusion. Asphaltene molecules with a large PAH emit red light and undergo slow diffusion.

The variation of the translational diffusion constant on the wavelength in FCS data is much more subtle. Rotational diffusion depends upon the cube of the molecular radius and therefore is very sensitive to compositional polydispersity, whereas the translational diffusion constant is linear in radius. In addition, the FCS experiments have been performed with long pass filters. Consequently, even for different excitation wavelengths, all fluorescent molecules contribute. On the other hand, the rotational diffusion measurements of asphaltene molecules used narrow excitation sources and emission filters. Consequently, the TRFD studies could pick out low quantum yield subsets of asphaltenes even in the presence of much stronger asphaltene fluorophores. Thus, the TRFD studies were designed to emphasize dispersion. The FCS studies here emphasize overall diffusion constants of bulk asphaltenes. The salient feature of the FCS vis-a-vis the TRFD studies is that the complaint that TRFD might suffer from extensive internal relaxation is shown to be incorrect. That is, TRFD and FCS diffusion constants are similar, showing that the internal rotation of chromophores is not significant in asphaltene molecules. Thus, asphaltenes cannot have loosely bound chromophores or internal relaxation could occur, which would produce large differences between rotational and translational diffusion constants. In addition, asphaltenes cannot have tightly bound different fused ring systems or there would be little dispersion in TRFD studies. Thus, asphaltenes predominantly have a single fused ring system per molecule.

Molecular Size and Weight. The FCS results herein and in refs 19 and 20 show that petroleum asphaltenes are comparable to molecules in the 750 Da range. The optical parameters of the asphaltene PAHs indicate there are on average about seven fused rings in asphaltene PAHs. If one combines one PAH of seven fused rings with 60% alkane carbon, then one obtains a molecule of 750 Da. Thus, the FCS result supports predominantly one PAH per molecule. Previous TRFD results^{12–14} and FCS results²⁰ show that coal asphaltenes are smaller than petroleum asphaltenes.^{12–14} Results shown in Table 2 support this contention. Coal asphaltenes have little alkane substituents, which produce steric repulsion and therefore must have small

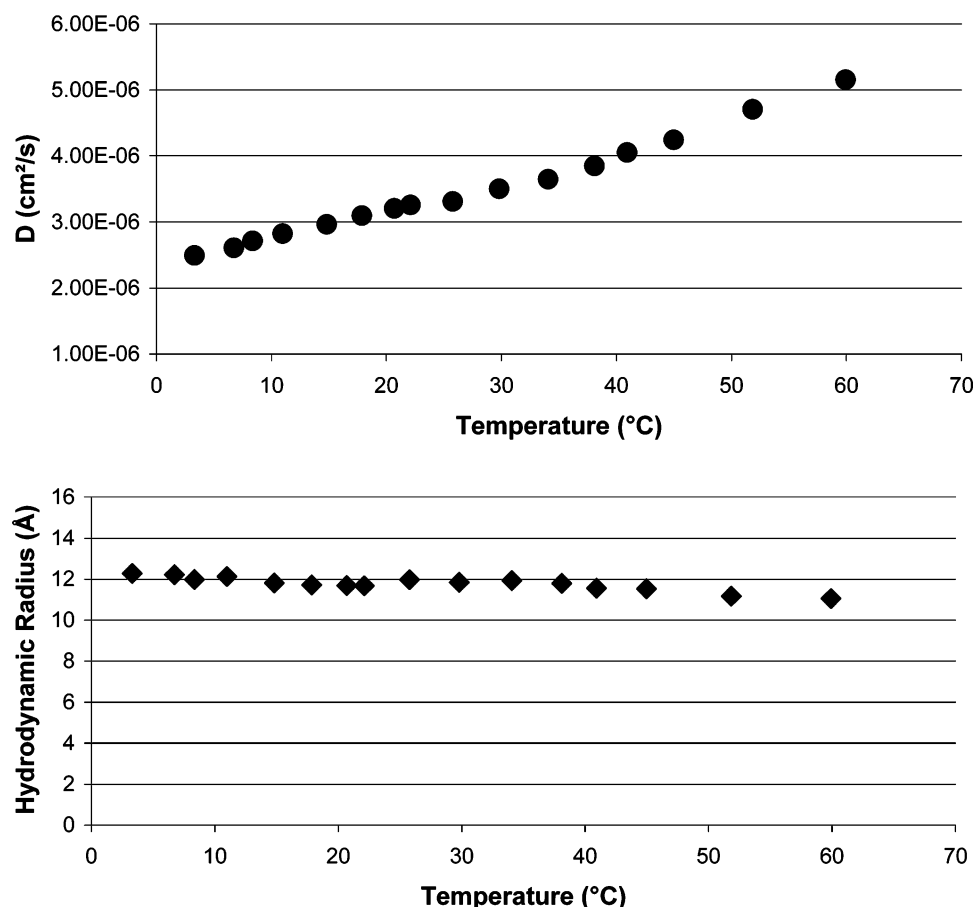


Figure 4. (a) Temperature dependence of diffusion coefficient D of BG5 asphaltene using the Peltier cooler as described in the text. (b) Hydrodynamic radius of BG5 calculated from measurements at various temperatures using temperature-dependent solvent viscosity from eq 5, which successfully accounts for almost all of the temperature dependence of D . The small temperature dependence of the hydrodynamic radius may correspond to a slight difference in the positioning of the alkane substituents.

Table 3. Comparison of Hydrodynamic Radii Determined by FCS and TRFD for Coal Asphaltene and Three Different Petroleum Asphaltenes^a

R_H (Å)	coal	CAL	UG8	ST1	porphyrin	QD
FCS (514 nm)	5.95	10.28	11.3	11.84	6.15 (TTB)	47.78
TRFD (530 nm) ¹⁰	8.65	11.35	12.05	12.85		
FCS (405 nm) ¹⁹			10.5			45.4
TRFD(406 nm) ¹⁰	5.7	7.85	9.0	10	6.05 (OEP)	

^a Because asphaltenes are a mixture of compounds, the different excitation wavelengths sample a different molecular component with differing molecular diameters. However, the QDs and porphyrins (TTB and OEP have similar masses and radii) are monodispersed and hence do not exhibit wavelength dispersion.

ring systems so that the van der Waals attraction is balanced by steric repulsion to maintain the same (asphaltene) solubility. Smaller ring systems and smaller alkane fractions couple to make coal asphaltene molecules smaller than those of petroleum asphaltenes. The balance of smaller repulsion and smaller attraction is mandated to keep fixed solubility per the definition of asphaltenes. It has been established that coal PAHs are smaller than petroleum PAHs by fluorescence emission spectroscopy¹⁴ and high-resolution transmission electron microscopy.²⁶

Table 2 even shows that the subtle molecular-weight differences in the model compounds are mostly reflected in the diffusion constants. FCS is a very sensitive tool to detect not only large molecular-weight differences between coal and crude oil asphaltenes but also a subtle difference between BPTI and BPTD for example. This sensitivity can be used to understand different petroleum asphaltenes.

The petroleum asphaltene with the smallest molecular size is the Cal asphaltene. This asphaltene is highly unusual in that it consists of a large fraction of sulfoxide.^{37,38} The sulfoxide group is likely to be alkyl sulfoxide.³⁷ As pointed out previously, the sulfoxide group has a dipole moment of 4 Debye and acts as a site of strong binding. To keep the asphaltene solubility constant with a site of strong binding, the other site of strong binding in the asphaltene molecule, the PAH, must be reduced in size. Because binding of PAHs scales with size, the smaller binding requirement of the Cal PAHs necessitates smaller chromophores and thus smaller molecules. The FCS results here are consistent with the TRFD results¹¹ that Cal asphaltene is the smallest virgin crude oil asphaltene that we have measured. Moreover, the blue-shifted fluorescence emission profile of Cal asphaltenes proves that the PAHs are smaller than normal for petroleum asphaltenes.¹¹

Conclusions

FCS has proven to be a valuable probe of asphaltenes. Interpretation of the FCS data in terms of a simple diffusion model has been tested under stringent conditions involving variations of temperature, asphaltene concentration, model compounds, and asphaltene type. The FCS results on transla-

(37) Waldo, G. S.; Mullins, O. C.; Penner-Hahn, J. E.; Cramer, S. P. Determination of the chemical environment of sulfur in petroleum asphaltenes by X-ray absorption spectroscopy. *Fuel* **1992**, *71*, 53–57.

(38) Mitra-Kirtley, S.; Mullins, O. C.; Ralston, C. Y.; Sellis, D.; Pareis, C. Sulfur speciation by XANES in maltenes, resins and asphaltenes and whole crude oils. *Appl. Spectrosc.* **1998**, *52*, 1522.

tional diffusion coefficients for a variety of asphaltenes and model compounds are in close accordance with those of rotational diffusion coefficients determined by TRFD. The large asphaltene diffusion coefficients confirm that asphaltenes are comprised of relatively small molecules. The strong correlation of the asphaltene molecular size with their spectral properties confirms that asphaltene PAHs constitute a significant fraction of the molecule. This mandates that asphaltene mol-

ecules possess one or two PAHs. Coal asphaltenes are shown to be smaller than petroleum asphaltenes, and a petroleum asphaltene rich in sulfoxide is smaller than other petroleum asphaltenes. These results are interpretable in terms of steric repulsion versus (van der Waals) attraction of fused aromatic ring systems.

EF700216R